# Towards wafer-scale 2D material sensors

Steeneken, P.G.; Soikkeli, M.; Pezone, R.; Vollebregt, S.; Houmes, M.J.A.; Verbiest, G.J.; Alijani, F.; Shin, D.; van der Zant, H.S.J.; More Authors

**Important note**
To cite this publication, please use the final published version (if applicable).
Please check the document version above.

**PERSPECTIVE • OPEN ACCESS**

# Towards wafer-scale 2D material sensors

View the article online for updates and enhancements.

## You may also like

# 2D Materials

# Towards wafer-scale 2D material sensors

Peter G Steeneken[1,*], Miika Soikkeli[2], Sanna Arpiainen[3], Arto Rantala[2], Raivo Jaaniso[4], Roberto Pezone[5], Sten Vollebregt[5], Sebastian Lukas[6], Satender Kataria[7], Maurits J A Houmes[8], Ruslan Álvarez-Diduk[9], Kangho Lee[10], Hutomo Suryo Wasisto[11], Sebastian Anzinger[11], Marc Fueldner[11], Gerard J Verbiest[1], Farbod Alijani[1], Dong Hoon Shin[1,12], Ermin Malic[13], Richard van Rijn[14], Tarja K Nevanen[2], Alba Centeno[15], Amaia Zurutuza[15], Herre S J van der Zant[8], Arben Merkoçi[9,16], Georg S Duesberg[10] and Max C Lemme[6,7]

1  Department of Precision and Microsystems Engineering, Delft University of Technology, Mekelweg 2, 2628 CD Delft, The Netherlands
2  VTT Technical Research Centre of Finland Ltd, PO Box 1000, FI-02044 VTT Espoo, Finland
3  Infineon Technologies AG, Wernerwerkstraße 2, 93049 Regensburg, Germany
4  Institute of Physics, University of Tartu, W. Ostwald Street 1, 50411 Tartu, Estonia
5  Microelectronics Department, Delft University of Technology, Mekelweg 4, 2628 CD Delft, The Netherlands
6  Chair of Electronic Devices, RWTH Aachen University, Otto-Blumenthal-Str. 25, 52074 Aachen, Germany
7  AMO GmbH, Advanced Microelectronic Center Aachen, Otto-Blumenthal-Str. 25, 52074 Aachen, Germany
8  Kavli Institute of Nanoscience, Delft University of Technology, 2628 CD Delft, The Netherlands
9  Nanobioelectronics & Biosensors Group, Institut Català de Nanociència i Nanotecnologia (ICN2), CSIC and the Barcelona Institute of Science and Technology (BIST), Campus UAB, Bellaterra, 08193 Barcelona, Spain
10  Institute of Physics & SENS Research Centre, University of the Bundeswehr Munich (UniBw M), Werner-Heisenberg-Weg 39, 85577 Neubiberg, Germany
11  Infineon Technologies AG, Am Campeon 1-15, 85579 Neubiberg, Germany
12  Department of Electronics and Information Engineering, Korea University, Sejong-ro 2511, Sejong 30019, Republic of Korea
13  Department of Physics, Philipps-Universität Marburg, Marburg, Germany
14  Applied Nanolayers B.V., Zilverstraat 1, 2718 RP Zoetermeer, The Netherlands
15  Graphenea, Paseo Mikeletegi 83, 20009 San Sebastián, Spain
16  ICREA Institució Catalana de Recerca i Estudis Avançats, Passeig de Lluís Companys, 23, 08010 Barcelona, Spain
*  Author to whom any correspondence should be addressed.

E-mail: p.g.steeneken@tudelft.nl

**Keywords:** 2D materials, sensor, graphene, NEMS, MEMS, waferscale, CMOS

## Abstract

The unique properties of two-dimensional (2D) materials bring great promise to improve sensor performance and realise novel sensing principles. However, to enable their high-volume production, wafer-scale processes that allow integration with electronic readout circuits need to be developed. In this perspective, we review recent progress in on-chip 2D material sensors, and compare their performance to the state-of-the-art, with a focus on results achieved in the Graphene Flagship programme. We discuss transfer-based and transfer-free production flows and routes for complementary metal-oxide-semiconductor integration and prototype development. Finally, we give an outlook on the future of 2D material sensors, and sketch a roadmap towards realising their industrial and societal impact.

## 1. Introduction

Sensor technology plays a key role in society, since it enables high-tech equipment and smart devices to monitor their environment. As a consequence of the increasing adoption of mobile devices and autonomous vehicles, sensors have become ubiquitous. With developments in artificial intelligence (AI), which facilitates fast interpretation of data from large sensor networks, the demand for small, low-cost, high-performance sensors continues to grow.

This trend was started by developments in microelectromechanical system (MEMS) technology, mainly in the period between 1990 and 2020, which have led to the integration of a large variety of MEMS sensors into almost every mobile phone, including accelerometers, gyroscopes, pressure sensors, magnetic field sensors, and microphones. The success of

these sensors is largely based on the possibility to produce them in large volumes on silicon wafers using manufacturing methods and tools that are also used in the semiconductor industry for fabricating complementary metal-oxide-semiconductor (CMOS) integrated circuits (ICs). The performance and production costs of many MEMS sensors have been industrially optimised. Hence, their cost and performance levels are currently close to limits imposed by physics, material properties, and production methods, making further improvements challenging.

Nevertheless, the discovery of graphene and other two-dimensional (2D) materials has opened up a route towards further advancing sensor technology beyond those limits for two key reasons. Firstly, 2D materials offer the opportunity to scale down layer thicknesses to a single atom. This substantially increases surface-to-volume ratio, which can enhance the sensitivity of a sensor layer to its environment. Secondly, the class of 2D materials features unique electronic, optical, mechanical and magnetic properties, enabling functionalities beyond what is offered by materials currently used in the semiconductor industry.

However, to realise this promise and bring 2D material sensors to the market, several challenges need to be dealt with. It needs to be proven, for each sensor technology, that 2D material sensors can outperform state-of-the-art sensors or can provide relevant sensor data that cannot be provided by current MEMS sensors. Moreover, it needs to be shown that reliable high-volume wafer-scale production of 2D material sensors is feasible, while also providing electronic readout. In the period between 2013 and 2023, a consortium of sensor groups have explored routes to deal with these challenges as part of the Graphene Flagship programme, funded by the European Commission. Here, we will provide a concise overview of the results of this exploration and provide a perspective on future developments in 2D material sensor technology, focusing on wafer-scale 2D sensors with electronic readout. This manuscript is thus not intended to provide a complete review of the field. We will first discuss wafer-scale integration methods, then give an outline of progress in wafer-scale 2D material sensors and finally provide a roadmap for 2D sensor development.

## 2. Wafer-scale 2D material integration for sensors

During the last two decades, the high-quality, wafer-scale growth of 2D materials [1] has received significant attention. Currently, (metal-organic) chemical vapour deposition (MOCVD) and plasma enhanced atomic layer deposition (PEALD) techniques have shown to provide wafer-scale 2D materials with quite good and uniform quality [2–4] on wafers with diameters up to 300 mm. Wafer-scale growth of a large number of 2D materials has been demonstrated [5]. However, further improvements in the material characteristics (including minimizing surface inhomogeneities and distortion), integration and cleaning methodologies are still required [6, 7]. This is especially true for 2D materials other than graphene which have been less extensively investigated. Here, we focus on the wafer-scale integration challenges for 2D material sensors fabrication.

### 2.1. Transfer-based and transfer-free 2D material integration

For realising wafer-scale process flows for 2D material sensors, an important question is whether to choose for a transfer-based flow, where the 2D material is grown on an optimised substrate and afterwards transferred onto the silicon wafer, or to choose a transfer-free process flow (also called direct-growth), where the 2D material is directly grown on the target wafer. Examples of wafers with 2D material for sensor applications are shown in figure 1.

A key difference between 2D material sensors and 2D material transistors is that sensors often need to be in contact with the environment. This makes it more attractive to integrate the 2D material on top of the back-end dielectrics and metals of a CMOS process, instead of near the front-end with silicon transistors.

Both transfer-free and transfer-based flows have been described in Lemme *et al* [10] and an example of a transfer-based CMOS integrated graphene device is shown in figure 2. Choosing between a transfer-based and transfer-free flow involves the following considerations. First of all, for transfer-free processes, the temperature at which the 2D material is grown needs to be low enough for the devices and interconnect on the wafer to remain undamaged. If there are back-end metals or interconnects, this limits growth temperatures to below 300 °C–400 °C. One example is $PtSe_2$ which can be grown well below 400 °C [11], by thermally assisted conversion (TAC) as shown in figure 1(d), which allows integration of $PtSe_2$ on Si waveguides [12, 13]. The material is suited for direct chemical sensing, piezoresistive devices, and IR detection [14, 15]. Secondly, a transfer-free approach often requires the seed layer, on which the 2D material is grown, to be specially deposited, and it sometimes needs to be removed after growth [16]. These constraints on transfer-free fabrication processes can sometimes also impact the quality of the grown 2D material layer. For some sensors, like microphones, it is custom in the industry to have a dedicated MEMS chip and separate application-specific IC for read-out which are packaged together (SiP, system-in-package). In these cases, a wider range of temperature and process conditions are possible, facilitating the use of transfer-free 2D materials.

Transfer-based process flows do not have these drawbacks, but on the other hand, they require a transfer procedure from the original growth substrate
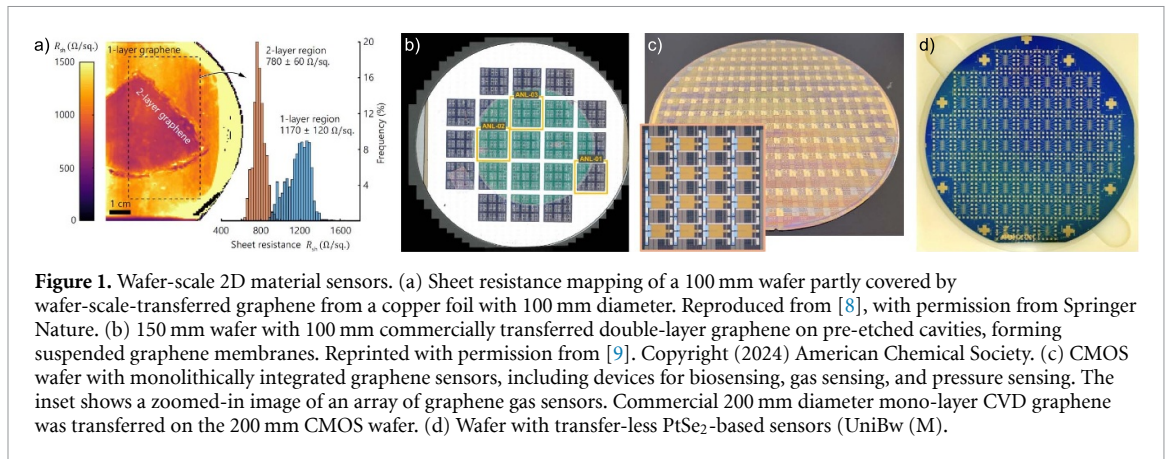
**Figure 1.** Wafer-scale 2D material sensors. (a) Sheet resistance mapping of a 100 mm wafer partly covered by wafer-scale-transferred graphene from a copper foil with 100 mm diameter. Reproduced from [8], with permission from Springer Nature. (b) 150 mm wafer with 100 mm commercially transferred double-layer graphene on pre-etched cavities, forming suspended graphene membranes. Reprinted with permission from [9]. Copyright (2024) American Chemical Society. (c) CMOS wafer with monolithically integrated graphene sensors, including devices for biosensing, gas sensing, and pressure sensing. The inset shows a zoomed-in image of an array of graphene gas sensors. Commercial 200 mm diameter mono-layer CVD graphene was transferred on the 200 mm CMOS wafer. (d) Wafer with transfer-less $PtSe_2$-based sensors (UniBw (M)).

to the target wafer of interest. This transfer procedure can cause contamination via residues from polymers and/or particles. Moreover, transferring the atomically thin layer without wrinkles and cracks, while preventing strain variations, is very challenging. Although both transfer-free and transfer-based flows have been shown to be feasible, there are still many challenges in optimising them and investigating their impact on device performance. The best choice for one of these flows will eventually depend on the type of device and its system integration with readout electronics.

By suspending 2D materials, improved sensitivity and new functions can be realised. However suspended 2D material sensors face the additional challenge of fabricating them without breaking the fragile membrane layer [10]. The feasibility of suspending atomically thin 2D materials with high yield using transfer has been demonstrated though, as seen in figure 1(b) [9]. Similarly, it has been demonstrated that nm-thin drums with diameters up to 155 $\mu$m can be realised with high yield using a transfer-free approach [17]. Finally, we note that irrespective of the choice of process flow, a key challenge is the development of process control and wafer-scale device yield methodologies, which for 2D material sensors often require unique techniques [18].

### 2.2. CMOS integration and electronic readout
Wafer-scale integration of 2D material sensors can enable their readout with CMOS ICs, as shown in figure 2. Such integration can be advantageous because it provides short electrical connections between the sensor and its readout circuit, resulting in small resistances and capacitances as well as immunity to external noise and interference. Furthermore it reduces the area and costs related to bondpads and bondwires in a multi-chip solution, in which the CMOS readout circuit would be on a chip that is separated from the sensor chip. Additionally, the demonstration of 2D material sensor integration with commercially available CMOS substrates increases the technology readiness level (TRL) and

moves 2D materials closer to potential industrial use [19]. Nevertheless, the trade-off between a monolithically integrated 2D material sensor on CMOS in a single chip and a system-in-package (SiP) multi-die solution with separate CMOS IC and sensor chips is not so easy to make. This trade-off is similar to that found in MEMS sensors [20].

Monolithic integration of CMOS and 2D materials increases process complexity, and can involve trade-offs in performance between 2D sensor and CMOS, in particular if the high-temperature steps of transfer-free 2D material growth impact CMOS performance. Moreover, from a cost perspective, the cost of a chip is usually determined by the number of process steps and/or masks, such that the monolithic solution can be more expensive, in particular when the CMOS IC area needed for readout is substantially different from the sensor area.

Nevertheless, for high-density sensor array applications, like in biosensors and gas sensors that require a high number of sensor elements for fingerprinting or statistically based sensing, the monolithically integrated solution is clearly preferable, since it substantially reduces the number of wirebonds and bondpads. A similar situation holds for CMOS integrated 2D material imaging sensors with high pixel densities [22], which are outside the scope of this perspective.

The CMOS IC design for readout of 2D material sensors requires a very good interaction between circuit designers and 2D material sensor device and process developers. To facilitate circuit design, it is helpful to develop compact models of the sensor devices [23], with good estimates of the model parameters. Making these estimates is sometimes challenging because the exact material and device parameters are often still unknown. The compact models are used by circuit designers in their simulators to verify and optimise their IC designs. IC circuit design for 2D materials is not fundamentally different than that for MEMS sensors, nevertheless challenges can appear in the details of the sensor readout, e.g. in cases where capacitances are very small or resonance frequencies very
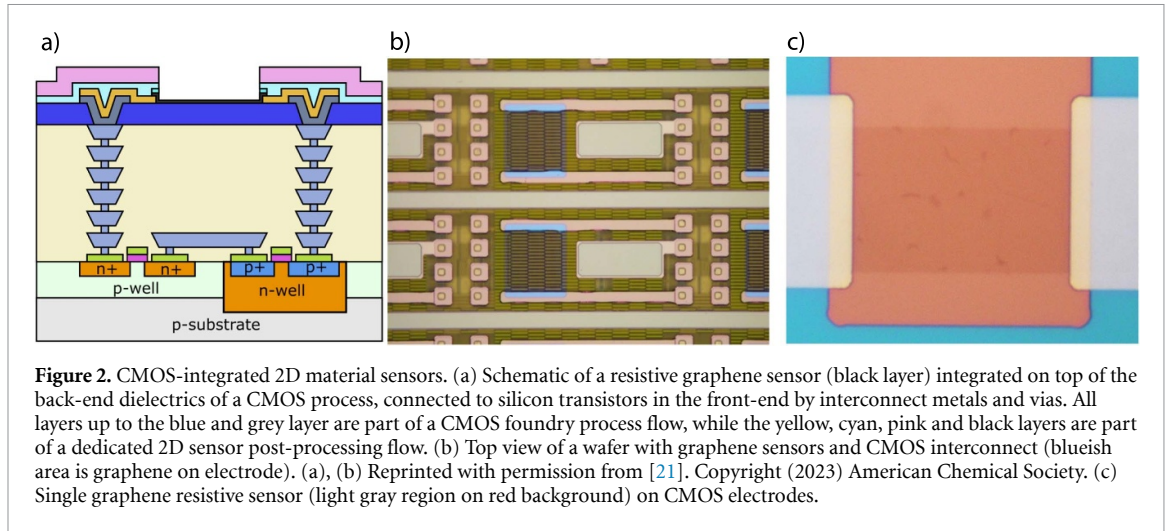
**Figure 2.** CMOS-integrated 2D material sensors. (a) Schematic of a resistive graphene sensor (black layer) integrated on top of the back-end dielectrics of a CMOS process, connected to silicon transistors in the front-end by interconnect metals and vias. All layers up to the blue and grey layer are part of a CMOS foundry process flow, while the yellow, cyan, pink and black layers are part of a dedicated 2D sensor post-processing flow. (b) Top view of a wafer with graphene sensors and CMOS interconnect (blueish area is graphene on electrode). (a), (b) Reprinted with permission from [21]. Copyright (2023) American Chemical Society. (c) Single graphene resistive sensor (light gray region on red background) on CMOS electrodes.

high. Furthermore, for sensor array readout, multiplexers [21] need to be designed to readout large numbers of sensor elements with a small number of bondpads.

After the circuit designs have been completed, CMOS wafers with these designs can be ordered from commercial foundries. Care must be taken to select a process that offers a sufficiently flat back-end surface planarity for transferring or growing 2D material. A large effort is the development of specialised backend processes to grow, transfer and pattern the 2D material sensors and for realising electrical connections between the 2D material sensors and the CMOS ICs (e.g. via the bondpads), like illustrated in figure 2(a). Finally, the CMOS chips with sensors and readout ICs are wirebonded in packages that are mounted on dedicated printed circuit boards (PCBs) with electronics for operating the sensors and transferring the sensor data.

## 3. 2D material sensors

In this section, we will discuss two classes of 2D sensors that have good potential for wafer-scale integration. Firstly, we discuss pressure sensors and microphones, which operate by detecting small changes in deflection of a suspended membrane. Secondly, we review gas and biosensors that operate by monitoring resistance changes of functionalised 2D material layers. Lastly, we conclude by discussing the value of prototypes in sensor research and development.
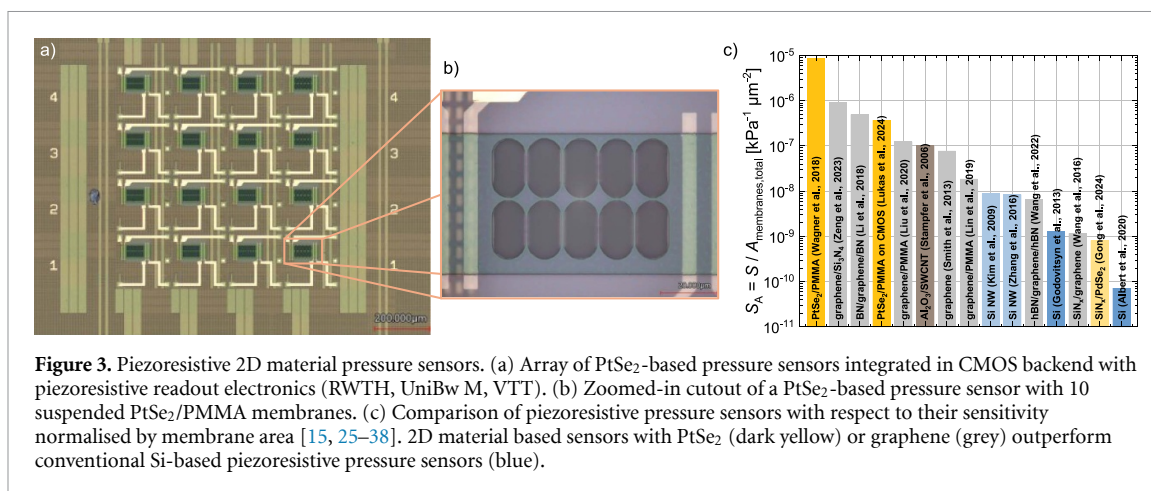
### 3.1. Pressure sensors and microphones
Since the bending rigidity of membranes scales proportional to the cube of their thickness $t$, 2D materials with atomic thickness can provide extremely flexible membranes. In fact, in contrast to most conventional MEMS sensors, 2D material membranes are often so thin that their pressure response is not governed by bending rigidity anymore, but is dominated by the membrane pretension $n_0$. In the linear regime, this pretension-limited operation results in a centre deflection [24] given by $\delta z = \frac{R^2}{4n_0}P$, where $R$ is the circular membrane radius and $P$ is the gas pressure difference across the membrane. Thus, 2D materials can be made much more sensitive to pressure than MEMS sensors by reducing pretension $n_0$ and increasing their radius $R$.

Pressure sensors and microphones are the most obvious sensor applications that can benefit from this high pressure sensitivity of 2D material membranes. Both sensor classes are of high interest because they address big markets, and are currently present in virtually every smart mobile device. Although both types of devices benefit from a high pressure sensitivity, other specifications are quite different. Pressure sensors should detect the absolute value of the static ambient pressure with high accuracy, with a precision down to ∼0.1 Pa. On the other hand, microphones need to provide low-noise detection of dynamic pressure variations over the audible frequency range (20 Hz–20 kHz), with a detection limit close to that of the human ear (20 $\mu$Pa).

For realising 2D material pressure sensors, two of the key challenges are hermetic sealing of high-yield membranes and providing high-resolution readout electronics for determining membrane deflection. Sealing the membrane is essential, since the sensor determines the ambient pressure by comparing it to the gas pressure in the sealed cavity. Therefore, the cavity pressure needs to be well-known and should not be time-dependent due to leakage through or along the 2D membrane. It is noted that the pressure of a sealed gas is temperature dependent according to the ideal gas law, although one can correct for this by using a temperature sensor and a temperature dependent calibration curve. Alternatively, it is possible to vacuum seal the cavity by the 2D material. Although 2D materials can provide very low leak rates [39], reaching high-yield hermetically sealed

**Figure 3.** Piezoresistive 2D material pressure sensors. (a) Array of PtSe$_2$-based pressure sensors integrated in CMOS backend with piezoresistive readout electronics (RWTH, UniBw M, VTT). (b) Zoomed-in cutout of a PtSe$_2$-based pressure sensor with 10 suspended PtSe$_2$/PMMA membranes. (c) Comparison of piezoresistive pressure sensors with respect to their sensitivity normalised by membrane area [15, 25–38]. 2D material based sensors with PtSe$_2$ (dark yellow) or graphene (grey) outperform conventional Si-based piezoresistive pressure sensors (blue).

cavities on wafer-scale is still an open challenge and might require dedicated postprocessing steps [40] for sealing.

For electronic readout of the pressure-induced deflection, two routes are available: capacitive and piezoresistive readout. Capacitive readout has the advantage that the capacitance between the membrane and the counter electrode is mainly determined by geometry, and is not significantly affected by material properties or potential contaminant particles on the 2D material. Although it has been shown [41] that pressure can be detected by a graphene membrane with a diameter of only 5 $\mu$m, the sensitivity of this sensor is less than 0.1 aF Pa$^{-1}$. Since state-of-the-art capacitive to voltage converters [42] have typical resolutions down to 4 aF, one would need at least 400 of these membranes to reach the required pressure resolution of 0.1 Pa, implying that the total device area is not much smaller anymore than MEMS pressure sensors. Further sensitivity improvement is possible by reducing the capacitive gap, however this impacts the sensing range. Thus, unless breakthrough innovations are made on capacitive readout of 2D material pressure sensors, it is at the moment unclear if they can ever substantially outperform state-of-the-art MEMS sensors that operate with larger area membranes.

Piezoresistive readout scales more favourably, since the signal is not proportional to the area of the sensor. Moreover, the discovery of 2D materials with very high piezoresistive gauge factors, such as PtSe$_2$ [15, 43], has boosted the performance of pressure sensors with piezoresistive readout. Good progress has been made in demonstrating pressure sensing with piezoresistive PtSe$_2$ sensors [27, 44], where high-sensitivity PtSe$_2$-based pressure sensors have been fabricated on CMOS substrates, as seen in figures 3(a) and (b). Open challenges remain the demonstration of hermetic sealing, dealing with cross-sensitivities and the nonlinear response of the sensors. It is noted that an alternative readout method is based on using the mechanical resonance

frequency for sensing. This method has successfully been demonstrated in graphene squeeze-film pressure sensors and microphones [45, 46] and benefits in particular from the low thickness and mass of 2D materials. Such resonant sensors will need dedicated CMOS integrated readout circuits [47].

The competition for 2D material pressure sensors consists of state-of-the-art commercial MEMS pressure sensors, like the Bosch BMP581, that utilises capacitive readout, and the earlier model Bosch BMP280 that uses piezoresitive readout and has a power consumption of only a few microwatts. The Bosch BMP581 provides a pressure noise of only 80 mPa, which allows it to detect altitude variations as small as 7 cm at sea level. Increasing sensitivity by using 2D materials might allow detecting even smaller pressure variations. Alternatively, since sensitivity scales with membrane area, it is possible to trade sensitivity for membrane area, providing similar sensitivity at smaller device footprint with dedicated 2D materials (see figure 3(c)).

The second class of membrane-based sensors are 2D material microphones, that need to provide resolutions in the $\mu$Pa range, which requires them to have larger areas than pressure sensors. However, reliably suspending monolayers or bilayers of 2D materials with diameters larger than 20–30 $\mu$m at wafer-scale has appeared to be very difficult. For that reason, most publications on 2D material microphones use thicker membranes. Recent studies have shown that transfer-free graphene multilayers, with thicknesses of 2–8 nm can provide large membranes, with diameters of more than a millimetre. These membranes have record sensitivities to sound [24] (orange hexagons in figure 4(b)) and also allow wafer-scale integration of capacitive readout electrodes and condenser backplates for capacitive readout of sound [48] (see figure 4(a)). A current challenge in 2D material microphones is dealing with the trade-off between sensitivity and bandwidth, which is more difficult for ultrathin membranes because air loading effects become substantial and push the fundamental
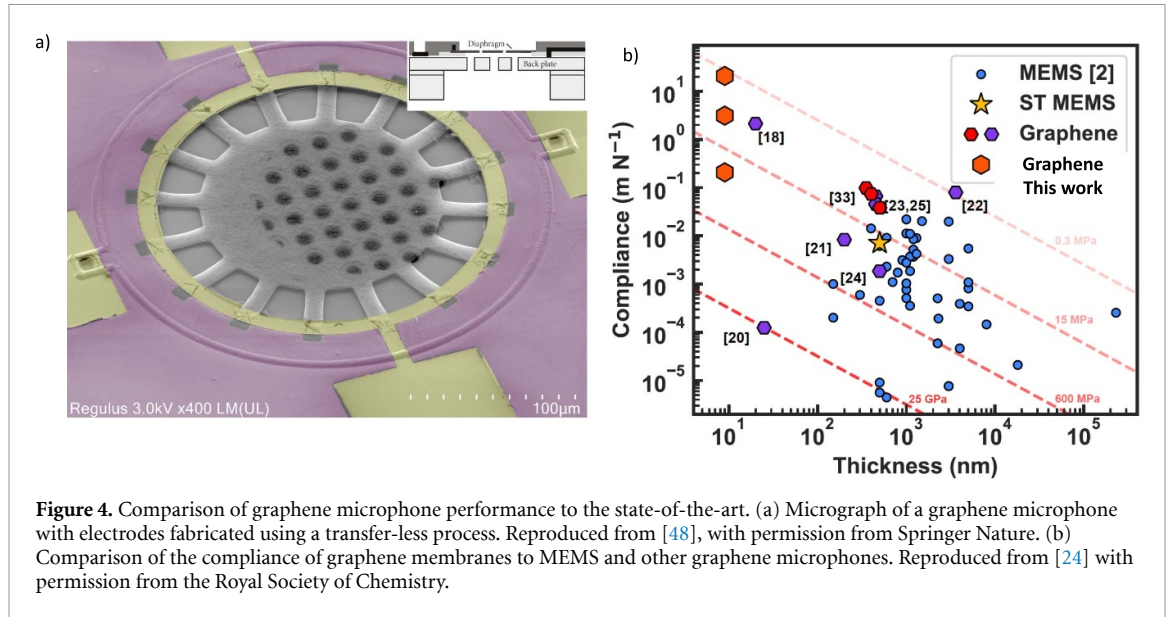
**Figure 4.** Comparison of graphene microphone performance to the state-of-the-art. (a) Micrograph of a graphene microphone with electrodes fabricated using a transfer-less process. Reproduced from [48], with permission from Springer Nature. (b) Comparison of the compliance of graphene membranes to MEMS and other graphene microphones. Reproduced from [24] with permission from the Royal Society of Chemistry.

resonance frequency down [49]. Furthermore, prototypes of 2D microphones with CMOS electrical readout need to be developed in order to benchmark their performance against state-of-the-art MEMS microphones [50]. Finally, microphones need to be robust against sudden pressure changes, a challenge that becomes more difficult to meet when thinning membranes down [49].

### 3.2. Gas and biosensors

The high-sensitivity electrical readout that 2D materials can offer [51, 52] for gas and biosensing is mainly based on their large surface-to-volume ratio. When a gas or biomolecule binds to this surface, the electron transfer or image charge formation can dope the 2D material and thus change the conductivity. Since the 2D material is only 1 atom thick, the resulting fractional resistance change is much larger than in a bulk material because the change in conductivity scales with the change in charge density and is thus inversely proportional to volume. It is therefore optimal to operate near the point where the intrinsic charge carrier density is lowest, which is the Dirac point in graphene. For that reason, bio and gas sensors are often using graphene field-effect transistors (FETs) whose operation point can be brought to the Dirac point with a gate electrode.

Two key challenges in gas and biosensing are obtaining good sensitivity and selectivity. In the field of gas and biosensors, the sensitivity (also called responsivity) of a linear sensor is usually defined as $\mathcal{S} = \frac{\Delta R}{R}\frac{1}{C}$, where $C$ is the gas or biomolecule concentration and $\Delta R = R(C) - R(0)$ is the change in resistance caused by the concentration increase. For improving detection of small concentration changes, it is both important to maximise sensitivity, and to minimise the intrinsic resistance fluctuations and noise of the sensor elements.

The challenge of enhancing selectivity, i.e. differentiating between different molecules, can be dealt with by creating arrays of 2D material sensor elements, where each of the sensor elements is functionalised by, or consisting of, a different layer of material. The specific sensitivity $\mathcal{S}_{ij}$ of each of the $N$ sensor elements is different and depends both on the type of gas/biomolecule $i$ and on the type of functionalisation material $j$. If such an array is exposed to a molecule $i=1$, the set of output signals from all of the sensor elements is proportional to $\mathcal{S}_{1j}$ with $j = 1 \ldots N$, which provides a fingerprint for molecule 1. For another molecule $i=2$ another fingerprint $\mathcal{S}_{2j}$ is obtained. To provide high selectivity, and distinguish molecules $i=1$ and 2, the sensitivities of the functionalisation layers $\mathcal{S}_{1j}$ and $\mathcal{S}_{2j}$ need to be sufficiently different. By increasing the number of differently functionalised sensor elements, and choosing the right functionalisation materials, more selectivity can be provided that can allow a higher number of molecules to be distinguished [53, 54].

To actually distinguish those molecules, the system requires to be calibrated or trained in a process where the sensitivities $\mathcal{S}_{ij}$ are established by sequentially exposing the sensor array to each of the different molecules $i$. For an ideal linear and additive system that is exposed to multiple gases with concentrations $C_i$, the output of each sensor element $S_j$ is then theoretically given by the equation:

$$S_j = \sum_i \mathcal{S}_{ij} C_i. \tag{1}$$

If the number of different sensor elements $N$ is equal to the number of different gases $M$, then the sensor signals $S_j$ can be used to determine the concentrations of all $M = N$ gases by solving this set of linear equations, if all rows in the sensitivity matrix $\mathcal{S}_{ij}$ are independent. In practice, the sensor response is

not linear and additive, such that more sophisticated algorithms based on principal component analysis and machine learning techniques [54] need to be applied to determine the molecular concentrations from multiple input signals after training.

Another important aspect is the response of the sensor in time. The absorption rate of molecules needs to be high enough to provide a stable signal within a specific time. Moreover, the sensing process needs to be reversible, and in some cases absorption and desorption rates are increased by increasing temperature with microheaters [54, 55], by light illumination [56, 57], or by using thin functionalisation layers to reduce diffusion times. Determination of the temperature at which absorption and desorption occurs might be used for increasing selectivity.

Multiplexed gas and biosensing arrays with graphene FETs on CMOS have been realised as discussed in [21] and shown in figure 2. Currently, a key challenge is to find methods and materials for functionalising them for sensitive and selective sensing. For detecting air pollution by gases like $NO_2$ and $O_3$, nanometre-thin metal oxide layers [54, 57] are promising candidates that can be deposited by pulsed laser deposition on the graphene FETs. The operation principle is based on the oxidising (electron addition) or reducing (electron removing) effect of gases on the metal oxide, where the graphene responds to the change in charge density.

An alternative approach to achieving selective sensing involves utilising 2D materials, such as transition-metal dichalcogenides (TMDs) directly as active channel in chemiresistive devices. This principle has been theoretically demonstrated in terms of the density of states (DOS) [58]. When integrating TMD materials onto Si substrates, TAC-derived TMD films with small crystallites offer several advantages. For instance, TAC-grown $MoS_2$ has shown high sensitivity to $NH_3$ even at sub-ppm levels [59]. Additionally, TAC-grown $PtSe_2$-based sensors exhibit both high sensitivity and rapid response time at room temperature [14]. Furthermore, the long-term stability of 2D material based sensors under ambient conditions has been often debated, but $PtSe_2$ film, even produced by liquid-phase exfoliation method, preserved gas sensitivity after 15 months or longer [57, 60]. Therefore, exploring various TMDs represents a promising pathway for achieving high sensitive and selective gas sensing [61, 62].

For biosensing, high specificity can be obtained using the antibody-antigen binding mechanism. To bind the antibody (or antigen) to the graphene surface both covalent and non-covalent binding strategies have been explored. Non-covalent binding has the advantage of better retaining the graphene's

intrinsic properties and has recently been used for direct functionalisation of the graphene FET surface by perylene bisimide (PBI) molecules [63, 64]. It is important to note the PBI molecules are applied before the wet chemical transfer of the graphene to the target substrate. The PBI form a stable self-assembled monolayer providing functional groups for subsequent functionalisation.

After amine-coupling of the antibody to the PBI, specific and sensitive detection of methamphetamine and cortisol was demonstrated [65]. The binding of these molecules to the antibody is accompanied by changes in the charge distribution near the graphene FET that alter its resistance. The big advantage of this technique is the high specificity of the antibody-antigen binding mechanism. Generally the functionalisation route can be employed to a wide range of specific targets. So far these types of sensors have been investigated only in single absorption measurements, which is useful for one-off test kits used for examples in road traffic controls. It remains to be determined if the sensors can be reused by flushing in buffer when kept in a liquid environment for continuous measurements. Further improvements in the selectivity of this type of graphene biosensors can be achieved by minimising non-specific absorption of molecules between or on top of the functionalisation molecules.

Besides wafer-scale sensors based on 2D GFETs, a large number of other types of 2D material biosensors have been investigated. Examples include vitamin $B_{12}$ or cholera toxin antigen plasmonic biosensors [66, 67], differential pulse voltammetry for dopamine detection [68], antibiotic susceptibility testing with graphene membranes [69], chemical sensing by 2D material excitons [70], and 2D electrodes for electrochemical biosensors [71].

As an example the fabrication of reduced graphene oxide (rGO) films embedded with metal nanoparticles (MNPs) via a one-step laser nanostructuration process offers an economical and scalable alternative for developing electrochemical biosensors, particularly for point-of-care (PoC) applications. This method, as described in [72], relies on a laser-induced co-reduction process that simultaneously reduces graphene oxide and metal cations to form highly exfoliated rGO nanosheets integrated with gold, silver, or platinum nanoparticles. The single-step process is versatile, requires minimal equipment, and eliminates the need for surfactants or complex procedures, making it a cost-effective solution. These rGO-MNP hybrid materials can be easily transferred onto any substrate, preserving their nanoarchitecture for reliable sensor performance (figure 5(a)).

Examples of such applications are widespread. For instance, rGO-AuNP hybrid electrodes produced
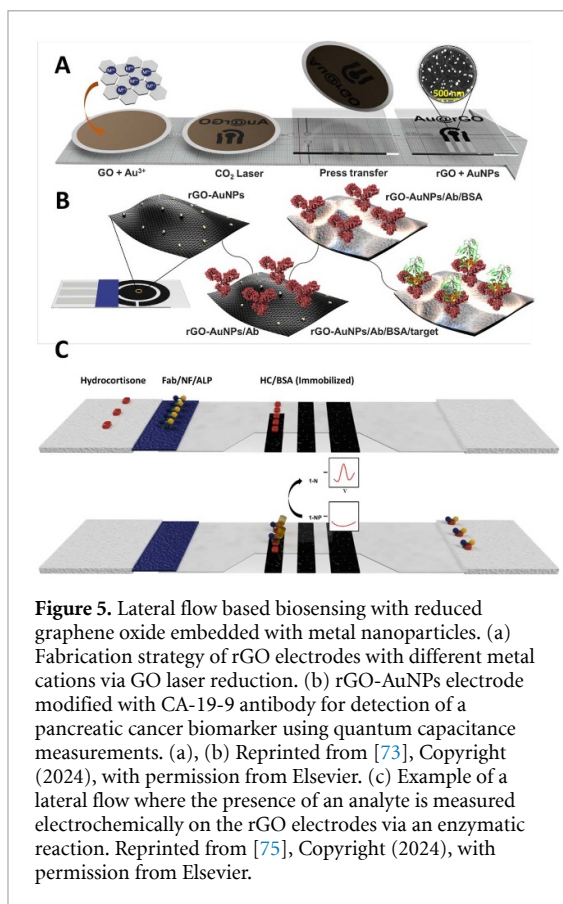
**Figure 5.** Lateral flow based biosensing with reduced graphene oxide embedded with metal nanoparticles. (a) Fabrication strategy of rGO electrodes with different metal cations via GO laser reduction. (b) rGO-AuNPs electrode modified with CA-19-9 antibody for detection of a pancreatic cancer biomarker using quantum capacitance measurements. (a), (b) Reprinted from [73], Copyright (2024), with permission from Elsevier. (c) Example of a lateral flow where the presence of an analyte is measured electrochemically on the rGO electrodes via an enzymatic reaction. Reprinted from [75], Copyright (2024), with permission from Elsevier.

via laser nanostructuring have been used for capacitive immunosensing, enabling the detection of cancer biomarkers, such as CA-19-9 glycoprotein (figure 5(b)), with high sensitivity and accuracy [73]. This sensor showcases its potential in clinical diagnostics, allowing label-free detection with a dynamic range from 0 to 300 U ml$^{-1}$, with a limit of detection of 8.9 U ml$^{-1}$. Another example is the use of a laser-assembled conductive 3D nanozyme film to detect hydrogen peroxide ($H_2O_2$) released by cancer cells in real time, highlighting the enzyme-free and low-cost nature of the process [74]. Furthermore, the integration of rGO electrodes into lateral flow assays (figure 5(c)) shows promise for scalable and advanced PoC diagnostics, overcoming the limitations of traditional electrode fabrication methods [75]. These studies collectively demonstrate the utility of this fabrication technique in various PoC biosensing applications.

### 3.3. Sensor prototypes

Although proof of principle demonstrations of 2D material sensors can often be provided in the lab with high-end measurement equipment, this only allows bringing the technology up to technology readiness level (TRL) 3–4. For increasing the maturity of the technology to TRL 5–6 and higher, it needs to be validated and demonstrated in a relevant and/or operational environment. For using and demonstrating sensor operation in such a relevant environment, the sensor, readout electronics, and data processing system need to be integrated in a portable prototype or demonstrator. For this purpose, having a wafer-scale sensor chip that can be read out electronically is highly beneficial, since electronic readout ICs and processors are relatively low-cost, low-power, and small. Compact sensor module prototypes can be realised on PCBs, powered by batteries and optionally be augmented by a wireless interface and display.

Examples, shown in figure 6, are a graphene capacitive pressure sensor prototype [42] and a graphene gas sensor array, functionalised by metal oxides with pulsed laser deposition, for detecting polluted gases [76]. The difficulty of designing, fabricating, and testing such a prototype strongly depends on the type of prototype and required performance. In general, the performance of the sensor when read out by low-cost electronics will be worse than when read out by high-end measurement equipment. However, in some cases reducing cable lengths and number of cables in a prototype can also provide advantages and performance increase, e.g. by reduction of parasitic capacitances.

Although realisation of stand-alone sensor prototypes can be time consuming and costly, and is not common practice in many scientific groups, it offers substantial advantages. The prototypes allow testing the technology in a relevant environment, which can provide valuable information on practical challenges like cross-talk with equipment, effect of harsh weather conditions, and user induced artifacts (e.g. affecting readings by touching the module). By making multiple low-cost prototypes, device-to-device variations can be assessed and stability and lifetime as a function of operational conditions can be assessed. Moreover, the prototypes can be shown at tradeshows and presentations not only to boost the confidence in the technology maturity, but also to attract companies and potential investors. This can reduce the threshold for bringing 2D material sensor technology to the market, either via adoption by industry or via start-up companies.

## 4. Roadmap and perspective

Twenty years after the discovery of graphene, and more than 10 years after starting the Graphene Flagship programme, significant progress has been
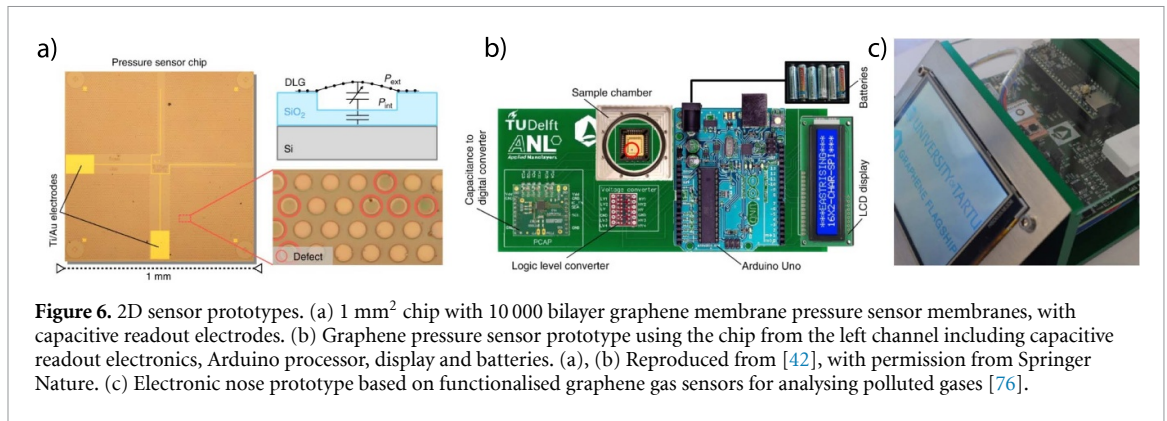
**Figure 6.** 2D sensor prototypes. (a) 1 mm$^2$ chip with 10 000 bilayer graphene membrane pressure sensor membranes, with capacitive readout electrodes. (b) Graphene pressure sensor prototype using the chip from the left channel including capacitive readout electronics, Arduino processor, display and batteries. (a), (b) Reproduced from [42], with permission from Springer Nature. (c) Electronic nose prototype based on functionalised graphene gas sensors for analysing polluted gases [76].
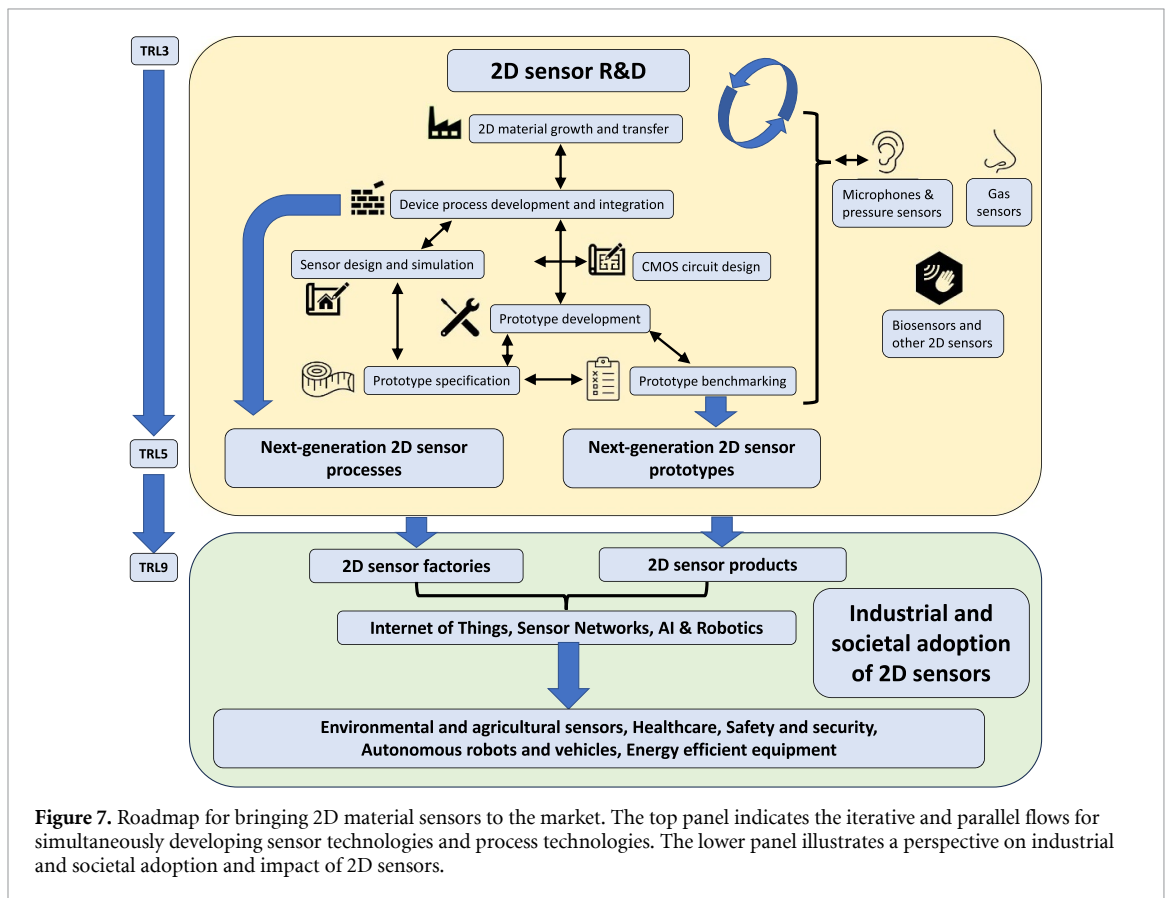


**Figure 7.** Roadmap for bringing 2D material sensors to the market. The top panel indicates the iterative and parallel flows for simultaneously developing sensor technologies and process technologies. The lower panel illustrates a perspective on industrial and societal adoption and impact of 2D sensors.

made in realising 2D material sensors, and processes to produce them on wafer-scale. Companies like Graphenea and Applied Nanolayers have realised wafer-scale 2D material production processes and several start-up companies have focused on developing 2D material sensors. Examples include QURV (wideband infrared image sensors) [22, 77], INBRAIN (brain-computer interface) [78], SoundCell (antibiotic susceptibility testing) [79], Paragraf (magnetic field sensors) and Grapheal (biosensors) [80, 81]. Nevertheless, although small-scale production has started, 2D material sensors, as far as

we know, do not seem to be in high-volume ($>$1 million products yr$^{-1}$) production at the moment.

As a future perspective, more work is needed to increase TRL and realise further industrialisation of 2D material sensors as indicated by the roadmap in figure 7. Several challenges run in parallel to expedite adoption of the technology by large companies in the semiconductor and sensor industries. First of all, stronger evidence is needed, theoretically and experimentally, that 2D material sensors can significantly outperform state-of-the-art sensors on *all or most* relevant performance parameters. Furthermore,

a reliable and scalable process flow needs to be developed for production of sensors at an acceptable cost-level. For optimising device performance, iteration loops are needed by which process flow parameters are optimised via experiments with device prototypes, and comparison to the state-the-art is performed. Test results are then used to improve design and process flows.

During this process, a key challenge is to bridge the gap between academic research and industrial product development. Companies would like to minimise risks as much as possible, and only after strong sensor performance of the module has been demonstrated at universities or at start-up companies, they will significantly increase investments in 2D sensor processes and product development. Once this gap towards industrial production has been bridged, large numbers of 2D sensors can be implemented in smart devices like phones, which will accelerate adoption of 2D sensor technology.

2D material sensors can then replace current sensors, and detect smaller signals with higher reliability at lower cost and power. 2D materials could also enable novel measuring principles, like single-molecule detection, to probe signals that cannot be detected with current sensors, leading to new products and application areas. Visionary examples include detection of diseases in plants using biosensors, using gas sensors to detect a person's health or contributing to personal identification by biometric sensors.

Eventually these 2D sensors, augmented by AI, can be integrated in Internet of Things (IoT) applications, sensor networks, autonomous vehicles and robotics. By applying the sensors in high quantities and densities, the technology will enable better monitoring of our environment, improving e.g. agricultural sensor networks and sensors for healthcare, and thus contribute to societal challenges like climate change, food and water scarcity. Based on these prospects, it is anticipated that 2D material sensor research will continue to grow and improve our lives in the upcoming years.

## Data availability statement

No new data were created or analysed in this study.

## Acknowledgments

## ORCID iDs

Peter G Steeneken ● https://orcid.org/0000-0002-5764-1218
Sten Vollebregt ● https://orcid.org/0000-0001-6012-6180
Sebastian Lukas ● https://orcid.org/0000-0002-8062-2832
Ruslan Álvarez-Diduk ● https://orcid.org/0000-0002-9876-1574
Kangho Lee ● https://orcid.org/0000-0002-6495-5231
Sebastian Anzinger ● https://orcid.org/0000-0002-6272-590X
Gerard J Verbiest ● https://orcid.org/0000-0002-1712-1234
Alba Centeno ● https://orcid.org/0000-0001-8442-2283
Arben Merkoçi ● https://orcid.org/0000-0003-2486-8085
Max C Lemme ● https://orcid.org/0000-0003-4552-2411

## References

[1] Xu X, Guo T, Kim H, Hota M K, Alsaadi R S, Lanza M, Zhang X and Alshareef H N 2022 *Adv. Mater.* **34** 2108258
[2] Asselberghs I *et al* 2020 *2020 IEEE Int. Electron Devices Meeting (IEDM)* pp 40.2.1–4
[3] Illarionov Y Y *et al* 2024 *npj 2D Mater. Appl.* **8** 8
[4] Lemme M *et al* 2025 *Nature Communications* **16** 1417
[5] Liu Z, Gong X, Cheng J, Shao L, Wang C, Jiang J, Cheng R and He J 2024 *Chip* **3** 100080
[6] Hallam T, Berner N C, Yim C and Duesberg G S 2014 *Adv. Mater. Interfaces* **1** 1400115
[7] Dong W, Dai Z, Liu L and Zhang Z 2024 *Adv. Mater.* **36** 2303014
[8] Quellmalz A *et al* 2021 *Nat. Commun.* **12** 917
[9] Lukas S *et al* 2024 *ACS Nano* **18** 25614
[10] Lemme M C *et al* 2020 *Research* **2020** 8748602
[11] Boland C S, Coileáin C O, Wagner S, McManus J B, Cullen C P, Lemme M C, Duesberg G S and McEvoy N 2019 *2D Mater.* **6** 045029
[12] Prechtl M *et al* 2021 *Adv. Funct. Mater.* **31** 2103936
[13] Parhizkar S *et al* 2022 *ACS Photonics* **9** 859–67
[14] Yim C *et al* 2016 *ACS Nano* **10** 9550
[15] Wagner S *et al* 2018 *Nano Lett.* **18** 3738
[16] Ricciardella F, Vollebregt S, Boshuizen B, Danzl F, Cesar I, Spinelli P and Sarro P M 2020 *Mater. Res. Express* **7** 035001
[17] Pezone R, Baglioni G, Sarro P M, Steeneken P G and Vollebregt S 2022 *ACS Appl. Mater. Interfaces* **14** 21705
[18] Cartamil-Bueno S J, Centeno A, Zurutuza A, Steeneken P G, van der Zant H S J and Houri S 2017 *Nanoscale* **9** 7559
[19] Lemme M C, Akinwande D, Huyghebaert C and Stampfer C 2022 *Nat. Commun.* **13** 1392
[20] Fischer A C, Forsberg F, Lapisa M, Bleiker S J, Stemme G, Roxhed N and Niklaus F 2015 *Microsyst. Nanoeng.* **1** 15005
[21] Soikkeli M *et al* 2023 *ACS Appl. Electron. Mater.* **5** 4925
[22] Goossens S *et al* 2017 *Nat. Photon.* **11** 366
[23] Li O, Xu Y, Wu Y, Guo Y, Zhang Y, Xu R and Yan B 2012 *2012 IEEE/MTT-S Int. Microwave Symp. Digest* (IEEE) pp 1–3
[24] Baglioni G, Pezone R, Vollebregt S, Cvetanović Zobenica K, Spasenović M, Todorović D, Liu H, Verbiest G J, van der Zant H S J and Steeneken P G 2023 *Nanoscale* **15** 6343
[25] Zeng S, Tang C, Hong H, Fang Y, Li Y, Wang Y, Kong L, Sun J, Zhu M and Deng T 2023 *IEEE Sens. J.* **23** 2008

[26] Li M, Wu C, Zhao S, Deng T, Wang J, Liu Z, Wang L and Wang G 2018 *Appl. Phys. Lett.* **112** 143502

[27] Lukas S *et al* 2024 Piezoresistive PtSe$_2$ pressure sensors with reliable high sensitivity and their integration into CMOS ASIC substrates accepted (https://doi.org/10.1021/acsnano.4c15098)

[28] Liu Y, Zhang Y, Lin X, Lv K-H, Yang P, Qiu J and Liu G-J 2020 *Micromachines* **11** 786

[29] Stampfer C, Helbling T, Obergfell D, Schöberle B, Tripp M K, Jungen A, Roth S, Bright V M and Hierold C 2006 *Nano Lett.* **6** 233

[30] Smith A D *et al* 2013 *Nano Lett.* **13** 3237

[31] Lin X, Liu Y, Zhang Y, Yang P, Cheng X, Qiu J and Liu G 2019 *Nano* **14** 1950130

[32] Kim J H, Park K T, Kim H C and Chun K 2009 *TRANSDUCERS 2009—2009 Int. Solid-State Sensors, Actuators and Microsystems Conf.* pp 1936–9

[33] Zhang J, Zhao Y, Ge Y, Li M, Yang L and Mao X 2016 *Micromachines* **7** 187

[34] Wang J, Xie C, Li M and Bai J 2022 *IEEE Trans. Electron Devices* **69** 4521

[35] Godovitsyn I V, Amelichev V V and Pankov V V 2013 *Sens. Actuators A* **201** 274

[36] Wang Q, Hong W and Dong L 2016 *Nanoscale* **8** 7663

[37] Gong Y, Liu L, Zhang R, Lin J, Yang Z, Wen S, Yin Y, Lan C and Li C 2024 *Nanotechnology* **35** 195203

[38] Albert S G, Luber S M and Winkler B 2020 *Handbook of Silicon Based Mems Materials and Technologies* (*Micro and Nano Technologies*) 3rd edn, ed M Tilli, M Paulasto-Krockel, M Petzold, H Theuss, T Motooka and V Lindroos (Elsevier) pp 915–35

[39] Bunch J S, Verbridge S S, Alden J S, Van Der Zande A M, Parpia J M, Craighead H G and McEuen P L 2008 *Nano Lett.* **8** 2458

[40] Lee M, Davidovikj D, Sajadi B, Siskins M, Alijani F, van der Zant H S J and Steeneken P G 2019 *Nano Lett.* **19** 5313

[41] Davidovikj D, Scheepers P H, van der Zant H S J and Steeneken P G 2017 *ACS Appl. Mater. Interfaces* **9** 43205

[42] Šiškins M *et al* 2020 *Microsyst. Nanoeng.* **6** 102

[43] Lukas S *et al* 2021 *Adv. Funct. Mater.* **31** 2102929

[44] Lukas S *et al* 2023 *2023 Device Research Conf. (DRC)* pp 1–2

[45] Dolleman R, Davidovikj D, Cartamil-Bueno S, van der Zant H S J and Steeneken P 2016 *Nano Lett.* **16** 568

[46] Abrahams M P, Martinez J, Steeneken P G and Verbiest G J 2024 *Nano Lett.* **24** 14162

[47] Wiesner M, Lindvall N and Yurgens A 2014 *J. Appl. Phys.* **116** 224510

[48] Pezone R, Anzinger S, Baglioni G, Wasisto H S, Sarro P M, Steeneken P G and Vollebregt S 2024 *Microsyst. Nanoeng.* **10** 27

[49] Pezone R, Baglioni G, van Ruiten C, Anzinger S, Wasisto H, Sarro P M, Steeneken P and Vollebregt S 2024 *Appl. Phys. Lett.* **124** 123503

[50] Fueldner M 2020 *Handbook of Silicon Based Mems Materials and Technologies* (*Micro and Nano Technologies*) ed M Tilli, M Paulasto-Krockel, M Petzold, H Theuss, T Motooka and V Lindroos (Elsevier) pp 937–48

[51] Pe na-Bahamonde J, Nguyen H N, Fanourakis S K and Rodrigues D F 2018 *J. Nanobiotechnol.* **16** 75

[52] Meng Z, Stolz R M, Mendecki L and Mirica K A 2019 *Chem. Rev.* **119** 478

[53] Kodu M, Lind M, Kiisk V, Renge I and Jaaniso R 2024 *Proceedings* **97** 165

[54] Lind M, Kiisk V, Kodu M, Kahro T, Renge I, Avarmaa T, Makaram P, Zurutuza A and Jaaniso R 2022 *Chemosensors* **10** 68

[55] Sacco L N, Meng H and Vollebregt S 2022 *2022 IEEE Sensors* (IEEE) pp 1–4

[56] Pe na A, Matatagui D, Ricciardella F, Sacco L, Vollebregt S, Otero D, López-Sánchez J, Marín P and Horrillo M C 2023 *Appl. Surf. Sci.* **610** 155393

[57] Berholts A, Kodu M, Rubin P, Kahro T, Alles H and Jaaniso R 2024 *ACS Appl. Mater. Interfaces* **16** 43827

[58] Sajjad M, Montes E, Singh N and Schwingenschlögl U 2017 *Adv. Mater. Interfaces* **4** 1600911

[59] Lee K, Gatensby R, McEvoy N, Hallam T and Duesberg G S 2013 *Adv. Mater.* **25** 6699

[60] Lee K *et al* 2023 *J. Mater. Chem.* **11** 593

[61] Zhao Y-F *et al* 2020 *Adv. Mater. Technol.* **5** 1901085

[62] Zhao Y, Wu G, Hung K-M, Cho J, Choi M, Coileáin C O, Duesberg G S, Ren X-K, Chang C-R and Wu H-C 2023 *ACS Appl. Mater. Interfaces* **15** 17335

[63] Berner N C, Winters S, Backes C, Yim C, Dümbgen K C, Kaminska I, Mackowski S, Cafolla A A, Hirsch A and Duesberg G S 2015 *Nanoscale* **7** 16337

[64] Winters S, Berner N C, Mishra R, Dümbgen K C, Backes C, Hegner M, Hirsch A and Duesberg G S 2015 *Chem. Commun.* **51** 16778

[65] von Lüders L, Tilmann R, Lee K, Bartlam C, Stimpel-Lindner T, Nevanen T K, Iljin K, Knirsch K C, Hirsch A and Duesberg G S 2023 *Angew. Chem., Int. Ed.* **62** e202219024

[66] Singh M, Holzinger M, Tabrizian M, Winters S, Berner N C, Cosnier S and Duesberg G S 2015 *J. Am. Chem. Soc.* **137** 2800

[67] Bareza N J, Wajs E, Paulillo B, Tullila A, Jaatinen H, Milani R, Dore C, Mihi A, Nevanen T K and Pruneri V 2023 *Adv. Mater. Interfaces* **10** 2201699

[68] Giacomelli C, Álvarez-Diduk R, Testolin A and Merkoçi A 2020 *2D Mater.* **7** 024006

[69] Rosłoń I E, Japaridze A, Steeneken P G, Dekker C and Alijani F 2022 *Nat. Nanotechnol.* **17** 637

[70] Feierabend M, Berghäuser G, Knorr A and Malic E 2017 *Nat. Commun.* **8** 14776

[71] Zhao L, Rosati G, Piper A, de Carvalho Castro e Silva C, Hu L, Yang Q, Della Pelle F, Alvarez-Diduk R R and Merkoçi A 2023 *ACS Appl. Mater. Interfaces* **15** 9024

[72] Scroccarello A, Álvarez-Diduk R, Della Pelle F, de Carvalho Castro e Silva C, Idili A, Parolo C, Compagnone D and Merkoçi A 2023 *ACS Sens.* **8** 598

[73] Echeverri D, Calucho E, Marrugo-Ramírez J, Álvarez Diduk R, Orozco J and Merkoçi A 2024 *Biosens. Bioelectron.* **252** 116142

[74] Bukhari Q U, Della Pelle F, Alvarez-Diduk R, Scroccarello A, Nogués C, Careta O, Compagnone D and Merkoci A 2024 *Biosens. Bioelectron.* **262** 116544

[75] Calucho E, Álvarez Diduk R, Piper A, Rossetti M, Nevanen T K and Merkoçi A 2024 *Biosens. Bioelectron.* **258** 116315

[76] Jaaniso R *et al* 2019 The University of Tartu develops a mobile sensor to sniff out toxic substances (available at: https://estonianworld.com/technology/the-university-of-tartu-develops-a-mobile-sensor-to-sniff-out-toxic-substances/)

[77] Akinwande D, Huyghebaert C, Wang C-H, Serna M I, Goossens S, Li L-J, Wong H-S P and Koppens F H 2019 *Nature* **573** 507

[78] Viana D *et al* 2024 *Nat. Nanotechnol.* **19** 514

[79] Rosłoń I, Japaridze A, Naarden L, Smeets L, Dekker C, van Belkum A, Steeneken P and Alijani F 2024 *Appl. Phys. Lett.* **124** 010501

[80] Schmaltz T, Wormer L, Schmoch U and Döscher H 2024 *2D Mater.* **11** 022002

[81] Urade A R, Lahiri I and Suresh K 2023 *JOM* **75** 614